JSHC
Japan Society of Histochemistry and Cytochemistry
Established 1959

Acta Histochem. Cytochem. 45 (5): 283–292, 2012
doi:10.1267/ahc.12012

Stimulation of Osteogenesis in Bone Defects Implanted with Biodegradable Hydroxyapatite Composed of Rod-Shaped Particles under Mechanical Unloading

Tohru Ikeda[1], Yoshinori Gonda[1,2,4], Eri Tatsukawa[1], Yasuaki Shibata[1], Masanobu Kamitakahara[3], Takatoshi Okuda[2], Ikuho Yonezawa[2], Hisashi Kurosawa[2,5] and Koji Ioku[3]

[1]Department of Oral Pathology and Bone Metabolism, Basic Medical Sciences Unit, Nagasaki University Graduate School of Biomedical Sciences, 1–7–1 Sakamoto, Nagasaki 852–8588, Japan, [2]Department of Orthopedic Surgery, School of Medicine, Juntendo University, 2–1–1 Hongo, Bunkyo-ku, Tokyo 113–8421, Japan, [3]Graduate School of Environmental Studies, Tohoku University, 6–6–20 Aramaki, Aoba-ku, Sendai, Miyagi 980–8579, Japan, [4]Present address: Department of Orthopedic Surgery, Juntendo University Urayasu Hospital, 2–1–1 Tomioka, Urayasu, Chiba 279–0021, Japan and [5]Present address: Department of Orthopedic Surgery, Juntendo Tokyo Koto Geriatric Medical Center, 3–3–20 Shin-suna, Koto-ku, Tokyo 136–3111, Japan

Received April 4, 2012; accepted July 13, 2012; published online September 8, 2012

The aim of this study was to evaluate the influence of mechanical unloading on the repair of bone defects with implantation of biodegradable bone substitutes. Spherical granules of biodegradable hydroxyapatite composed of rod-shaped particles (RHA) or beta-tricalcium phosphate composed of rod-shaped particles (RTCP) were implanted into a bone defect created in the distal end of the right femur of 8-week-old Wistar rats. Two, 6, 10, and 22 weeks after implantation, part of the sciatic nerve in the thigh was resected and exposed to mechanical unloading for 2 weeks. Then, 4, 8, 12 and 24 weeks after implantation, repair of the bone defect was analyzed. As a control, the bone defect without implantation of ceramic granules was also analyzed. Both RHA and RTCP tended to be reduced, but the reduction was not obvious during the experimental period. At 12 and 24 weeks after implantation, the amount of newly formed bone in the animal implanted with RHA was significantly greater than that at 4 weeks after implantation, but that in the animal implanted with RTCP or without implantation was not significantly different. The number of osteoclasts in the region implanted with RHA was significantly larger than that of the region implanted with RTCP or without implantation at 12 and 24 weeks. The activities of alkaline phosphatase in osteoblasts and tartrate-resistant acid phosphatase in osteoclasts were remarkably increased in the bone defects with implantation compared with those in the bone defects without implantation. These results suggested that RHA stimulated osteogenesis and osteoclastogenesis even after 2 weeks of mechanical unloading, and that RHA could be expected to improve the repair of bone defects in patients under the condition of skeletal unloading.

Key words: mechanical unloading, bone substitute, hydroxyapatite, beta-tricalcium phosphate, bone metabolism

Correspondence to: Tohru Ikeda, DDS, Ph.D., Department of Oral Pathology and Bone Metabolism, Basic Medical Sciences Unit, Nagasaki University Graduate School of Biomedical Sciences, 1–7–1 Sakamoto, Nagasaki 852–8588, Japan.
E-mail: tohrupth@nagasaki-u.ac.jp

I. Introduction

Mechanical unloading has been shown to reduce bone mass through analyses of the bone after space flights [3, 7, 26, 33, 37] and animal experiments of skeletal unloading by sciatic neurectomy [19, 34, 41, 44], tail-suspension [10]

and tenotomy [43]. The biological mechanisms of reduction in bone mass under mechanical unloading are not completely understood, but they are thought to be caused by the inhibition of the bone-forming activity of osteoblasts and/or stimulation of bone resorption by osteoclasts [10, 24, 26, 43]. It was also reported that bisphosphonates prevented bone loss induced by tail suspension or sciatic neurectomy using animal models, and reduction of bone mass under mechanical unloading was suggested to be effectively prevented by attenuation of osteoclasts [2, 4, 27]. The biological functions of osteocytes remain largely unclear, but osteocytes are suggested to contribute widely to various phenomena from bone formation to bone resorption [8, 18]. In addition, osteocytes were strongly suggested to play important roles to transmit mechanical force to other cells and to regulate mineral homeostasis [8]. Recent studies strongly suggested that osteocytes play a key role in the reduction in bone mass under mechanical unloading through the regulation of osteoclastogenesis [36, 45]. From these studies, loss of bone mass induced by skeletal unloading is speculated to be caused by stimulated osteoclastic resorption of bone under conditions of reduced osteogenic activity, and osteocytes to be associated with induction of aberrant bone metabolism.

To improve the healing of bone defects, autologous bone grafts have long been used, and more recently, bone substitutes have also been applied for implants to fill bone defects in the fields of orthopedic surgery and dentistry. Hydroxyapatite (HA) is known to exhibit potent osteoconductivity and has been used as a bone substitute [6, 14, 23]. HA is also known as a ceramic with an unbiodegradable nature when implanted into the bone, although a few reports have suggested that HA is resorbed into bone [12]. Beta-tricalcium phosphate (β-TCP) is another bone substitute that has been frequently used recently because of its biodegradable nature [1, 22]. We have developed HA and β-TCP, composed of unique rod-shaped particles, using the applied hydrothermal method [16, 17]. Animal experiments showed that hydroxyapatite composed of rod-shaped particles (RHA), prepared using the applied hydrothermal method, had a mildly biodegradable nature, in contrast to stoichiometric HA that lacked biodegradability, and also had a stimulatory effect on osteogenesis [11, 31]. Previously, we found that β-TCP composed of rod-shaped particles (RTCP), prepared using the applied hydrothermal method, had more adequate biodegradability than conventional β-TCP composed of globular particles. When implanted into rabbit femurs, excess biodegradation of conventional β-TCP, composed of globular particles, caused the healing of bone defects with less bone than in animals implanted with RTCP [30].

Mechanical unloading significantly reduced bone mass during short periods (usually up to 2 weeks) [10, 21], and it may also affect the repair of bone defects with implantation of bone substitutes. However, the regenerative potential of bone defects under mechanical unloading is poorly understood, and only limited reports have suggested that immobilization delayed healing of bone defects [38, 40]. Moreover, the effect of mechanical unloading on biodegradable bone substitutes remains unknown. A condition corresponding to mechanical unloading takes place under long-term bed rest, hence the evaluation of the repair of bone defects implanted with biodegradable bone substitutes under mechanical unloading is important. Considering the importance of osteocytes for bone loss caused by mechanical unloading [36, 45], biodegradation of bone substitutes might be independent of mechanical unloading and only newly formed bone might be affected. During the repair process of a bone defect, hybrid hard tissue composed of residual bone substitutes and newly formed bone is formed [11], and the ratio of remaining bone substitutes and newly formed bone changes according to the process of repair of bone defects. Hence, the effect of mechanical unloading might be affected by this ratio. To evaluate the effect of mechanical unloading on the repair of bone defects with implantation of biodegradable bone substitutes, we assessed the effect of 2 weeks of mechanical unloading on the repair of bone defects at 4, 6, 12 and 24 weeks after implantation of RHA or RTCP into rat femurs.

II. Materials and Methods

Preparation of ceramics

Alpha-TCP powder (Taihei Chemical Ind. Co. Ltd., Osaka, Japan) was mixed and kneaded with 10% gelatine solution, and dropped into a stirred oil bath heated to 80°C. The bath was then chilled on ice and spherical α-TCP/gelatine granules were formed. The granules were separated from the oil, rinsed and sintered at 1200°C for 10 min to remove gelatine and to maintain the crystal phase of α-TCP. The formed α-TCP granules were set in a 105 cm^3 autoclave at 160°C under saturated water vapor pressure for 20 hr [35]. Synthesized RHA granules were sieved and granules 0.5 to 0.6 mm in diameter were used for experiments. Spherical RTCP granules were prepared by further heating of RHA granules at 900°C for 3 hr for preparation of β-TCP [17]. The porosity of RHA and RTCP granules was designed to be 70%. Rod-shaped particles of spherical RHA granules and spherical RTCP granules were confirmed using a scanning electron microscope (SU8000, Hitachi, Ltd., Tokyo, Japan) (Fig. 1). Synthesized RHA and RTCP granules were analyzed by powder X-ray diffractometry with graphite-monochromatized CuKα radiation, operating at 40 kV and 40 mA (XRD; RINT-2200VL, Rigaku, Tokyo, Japan). We confirmed that the main phases of RHA and RTCP were HA and β-TCP, respectively (Fig. 2).

Animals and operative procedures

Eighty-four female 8-week-old Wistar rats were anesthetized with an intraperitoneal injection of ketamine (40 mg/kg body weight) and xylazine (3 mg/kg body weight) before surgery. Under sterile conditions, a dead-end bone defect 2 mm in diameter and 3 mm in depth was created in the medial cortex of the distal end of the right femur just

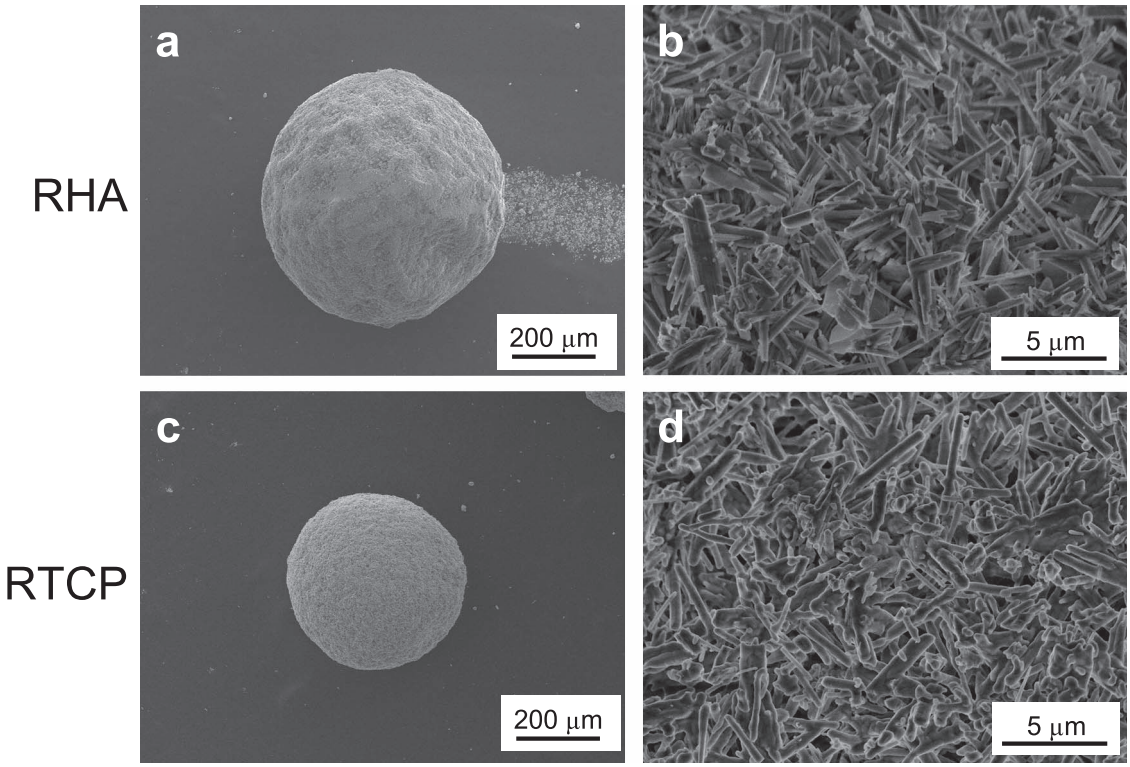

Fig. 1. Scanning electron micrographs of the overview (**a, c**) and the microstructure (**b, d**) of RHA (**a, b**) and RTCP (**b, d**) granules.

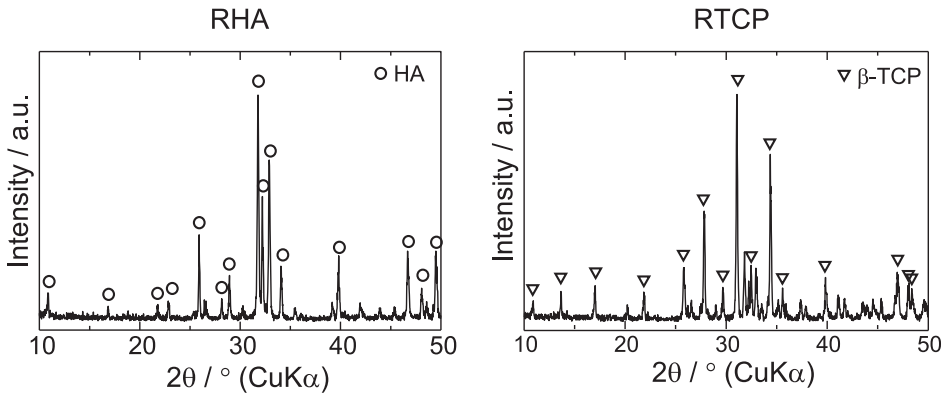

Fig. 2. X-ray diffractometry (XRD) of implants used in this study. From XRD patterns, RHA and RTCP granules were assigned to HA and β-TCP, respectively.

proximal to the epiphyseal growth plate using a Kirschner wire. The orientation of the defect was perpendicular to the sagittal axis of the femur. The defect was irrigated with saline, 30 mg of RHA or RTCP granules was implanted into the defect, and the wound was sutured layer by layer. Operated animals without implantation were used as a control. Two, 6, 10 and 22 weeks after operation, the sciatic nerve of the right thigh was cut and 2 mm in length was removed following a previous study with minor modifications [28]. After sciatic neurectomy, mechanical unloading of the right hind limb by paralysis was confirmed on the next day. Two weeks after sciatic neurectomy, animals were euthanized and the right femur and the tibia were resected (Fig. 3A). Sham operation of sciatic neurectomy was performed at 2 and 22 weeks after creation of the bone defect for some of the animals without implantation to evaluate the effects of sciatic neurectomy on bone. Six animals were used for each experimental group. Animal rearing and experiments were performed at the Biomedical Research Center, Center for Frontier Life Sciences, Nagasaki University, following the Guidelines for Animal Experimentation of Nagasaki University (Approval No. 0703010564).

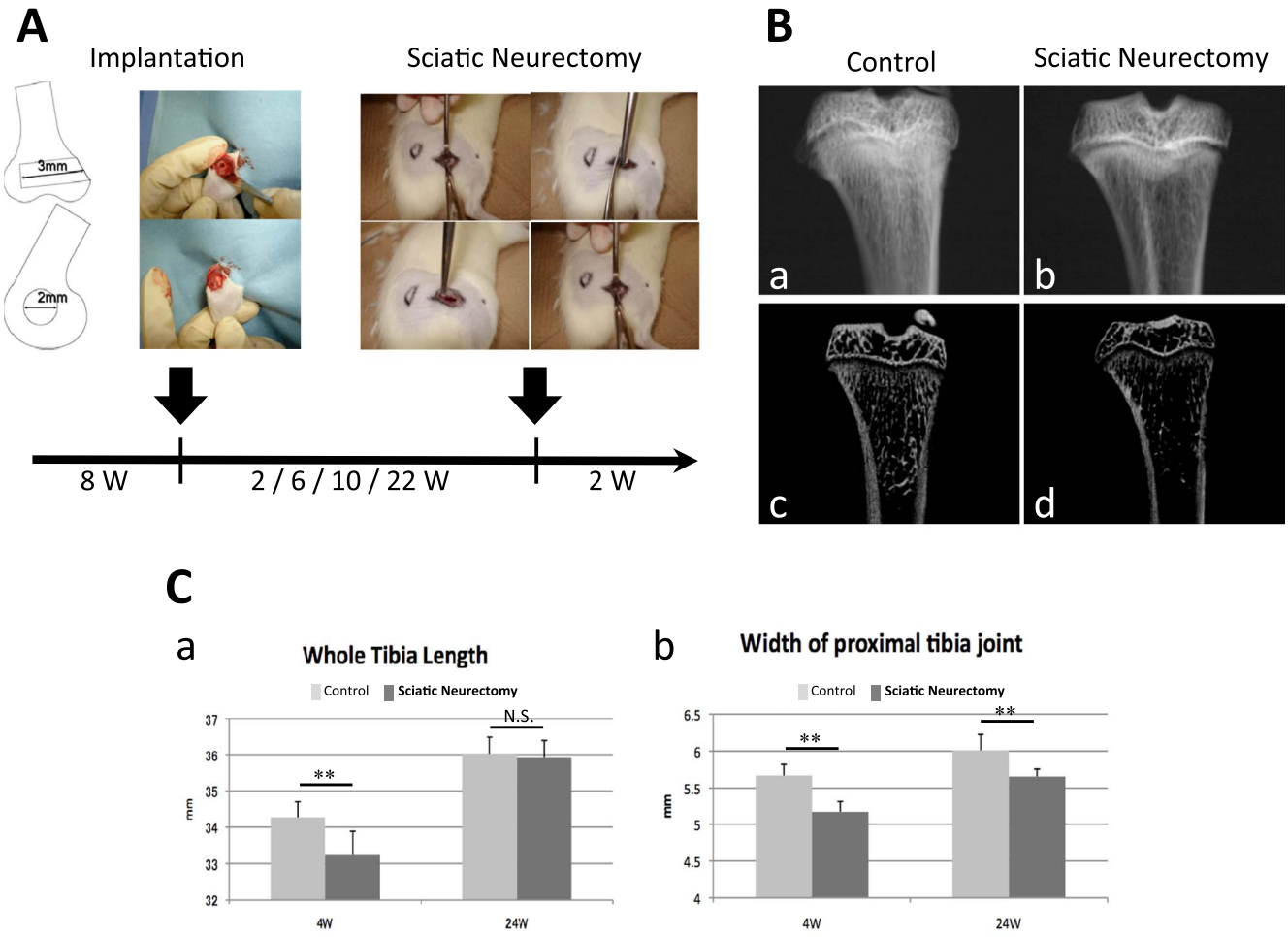

Fig. 3. Perioperative views of implantation and sciatic neurectomy (**A**), and effects of sciatic neurectomy on bone (**B, C**). (**B**) Representative views of the right tibia of an animal with sham operation for sciatic neurectomy (a, c) and with sciatic neurectomy (b, d) by simple X-ray analysis (a, b) and micro-CT analysis (c, d). Photographs were taken for tibiae at 4 weeks after creation of the bone defect in the femur. (**C**) Results of measurements with a caliper of the length (a) and the width of the proximal joint (b) of the tibiae at 4 weeks and 24 weeks after creation of the bone defect in the femur.

Radiological and histological analyses

Resected right tibiae were fixed in 4% formaldehyde in 0.1 M phosphate buffer (pH 7.2) at 4°C for 24 hr and stored in 70% ethanol at 4°C until micro-CT analysis. Micro-CT analysis was performed using an *in vivo* micro-X-ray CT system (R_mCT; Rigaku, Tokyo, Japan). Resected right femurs were fixed as described above, dehydrated, embedded in 2-hydroxyethyl methacrylate/methyl methacrylate/2-hydroxyethylacrylate mixed resin and sectioned at 3 µm thickness using adhesive films [30]. These sections were stained by the Giemsa method or histochemically stained for alkaline phosphatase (ALP) activity or tartrate-resistant acid phosphatase (TRAP) activity. TRAP activity was stained as described previously [15]. Staining for ALP activity was performed using 0.2 M Tris-HCl buffer (pH 8.5) as a reaction buffer. In this study, fast blue BB salt (F3378; Sigma, St. Louis, MO, USA) and fast red RC salt (F5146; Sigma) were used as couplers to detect ALP and TRAP activities, respectively. Sections stained for ALP activity and TRAP activity were counterstained with nuclear fast red and hematoxylin, respectively.

Histomorphometric analyses were performed using the Osteoplan II system (Carl Zeiss, Thornwood, NY, USA). In addition to standard parameters [32], original parameters were also used to analyze bone substitutes. The amount of residual implants and newly formed bone was evaluated using the following parameter: “Bone volume + implant volume over tissue volume” ([BV + Imp.V]/TV, %). The amount of residual implant was evaluated using the parameter “implant volume over tissue volume” (Imp.V/TV, %), the amount of newly formed bone was evaluated using the parameter “bone volume over tissue volume” (BV/TV, %) and the number of osteoclasts along the bone perimeter (N.Oc/B.Pm, per 100 mm) was also calculated. Histomorphometry was performed for each sample in a 0.6 mm×1.8 mm square, which was aligned on the medial longitudinal

axis of the femur and arranged centrally in the created bone defect following our previous study [11]. Osteoclasts were defined as multinucleated cells in contact with the bone or bone substitutes. Data are expressed as the mean±S.D. Statistical differences were evaluated with the *t*-test and *P* value <0.05 was considered significant.

III. Results

Effect of sciatic neurectomy on the bone

At 8 weeks of age, a bone defect was created in the distal end of the right femur of Wistar rats and implanted with bone substitutes; no implantation was made as a control. Then, the right sciatic nerve was resected at 2, 6, 10 and 22 weeks after implantation or creation of the bone defect. Some of the animals without implantation were sham-operated for sciatic neurectomy at 2 and 22 weeks after creation of the bone defect. All the animals were euthanized at 2 weeks after sciatic neurectomy or sham operation for sciatic neurectomy (Fig. 3A). Radiological findings of the right tibia of animals euthanized at 4 weeks after creation of the bone defect showed that, in both X-ray and micro-CT photographs, reduced trabecular bones were evident in animals with sciatic neurectomy compared with those with sham operation (Fig. 3B, a–d). In micro-CT photographs, reduced thickness of the cortical bone was also evident in animals with sciatic neurectomy (Fig. 3B, c, d). The right tibiae of animals with sciatic neurectomy were significantly shorter than those of animals with sham operation at 4 weeks after creation of the bone defect, but no significant difference was detected in animals at 24 weeks after creation of the bone defect (Fig. 3C, a). The width of the proximal joint of right tibiae of animals with sciatic neurectomy was significantly smaller than that of animals with sham operation at 4 and 24 weeks after creation of the bone defect (Fig. 3C, b).

Histological findings

Repair of bone defect was recognized in the marginal region of the defect at 4 weeks after its creation in animals without implantation (Fig. 4a). At 8 weeks after creation of the bone defect, repair with newly formed bone was predominantly seen in its central region in animals without implantation (Fig. 4b). At 12 and 24 weeks after creation of the bone defect, newly formed bone seen in its central region at 8 weeks after creation of the bone defect had been resorbed and was healed with thin trabecular bones and fatty bone marrow tissue in animals without implantation

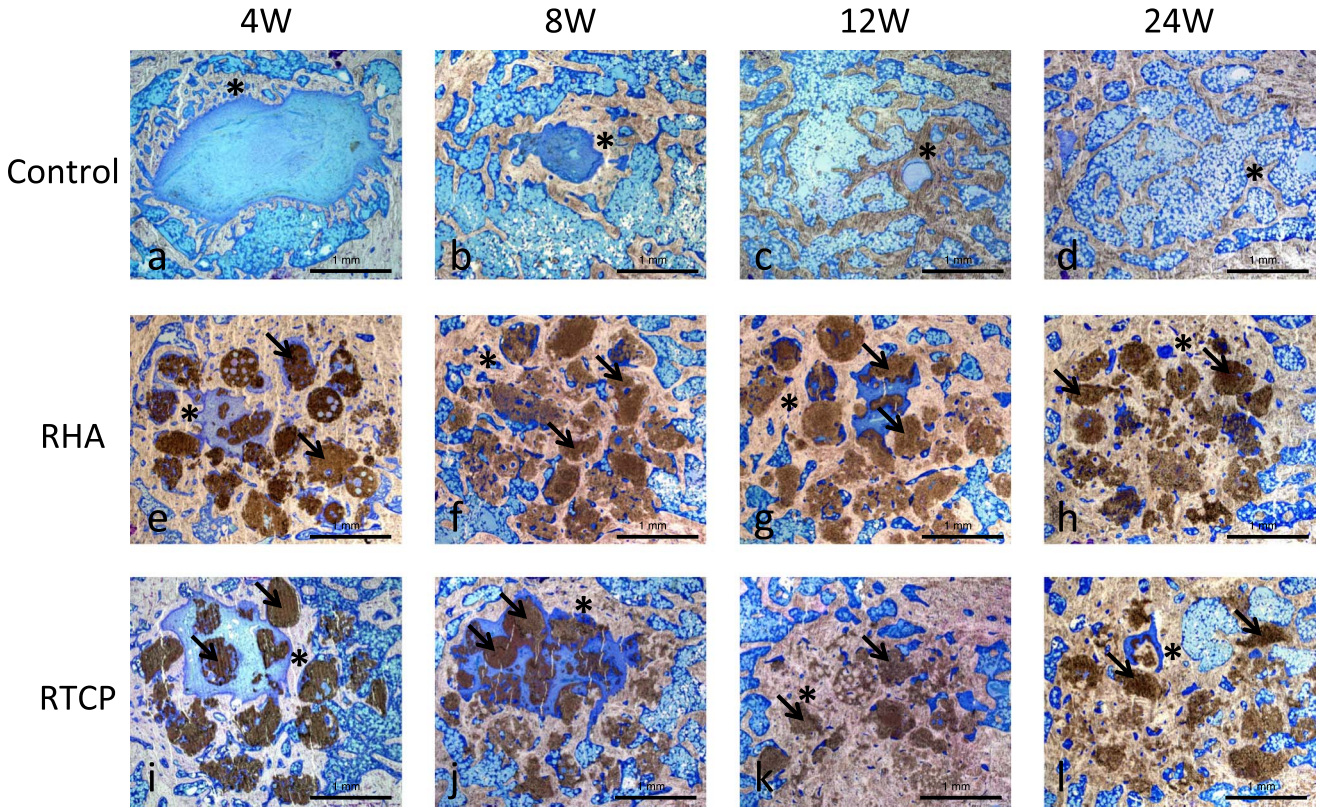

Fig. 4. Histological appearance of undecalcified sections of rat femurs without implantation (**a–d**), implanted with RHA (**e–h**) and implanted with RTCP (**i–l**). Sections were stained by Giemsa's method. Implants (arrows) were dark, bones (*) were whitish and soft tissues were blue in the specimen. A large number of residual ceramic granules, some of which were distorted in the implanted region during the healing process, were seen in animals implanted with RHA (**e–h**) or RTCP (**i–l**). Total amount of hard tissue including residual ceramic granules and newly formed bone was much larger than the amount of newly formed bone in animals without implantation.

(Fig. 4c, d). With bone substitutes, newly formed bone was widely distributed in the bone defect along the implanted bone substitutes at 4 weeks after implantation compared with that of animals without implantation (Fig. 4a, e, i). In contrast to animals without implantation, thick hybrid hard tissue composed of newly formed bone and residual ceramic granules was evident at 8, 12 and 24 weeks after implantation, and few thin trabecular bones were seen (Fig. 4f, g, h, j, k, l). Deformation of spherical ceramic granules was evident later than 8 weeks after implantation (Fig. 4g, h, k, l).

The activities of ALP and TRAP were analyzed by histochemical procedures. At 4 weeks after implantation or creation of the bone defect, osteoblasts with potent ALP activity were abundantly seen in osteoblasts on the surface of newly formed bone and some of the mesenchymal stromal cells in the bone marrow area (Fig. 5a, c, e). In animals without implantation at 24 weeks after creation of the bone defect, faint ALP activity was detected in a few lining cell-like flat-shaped osteoblasts on the surface of newly formed bone (Fig. 5b). In contrast to that in animals without implantation, many osteoblasts with potent ALP activity were detected on the surface of newly formed bone and in the bone marrow area of animals at 24 weeks after implantation of bone substitutes (Fig. 5d, f). TRAP-positive multinucleated cells were seen on the surface of bone substitutes or newly formed bone at 4 weeks after implantation or creation of the bone defect. The number of TRAP-positive cells in animals without implantation was much smaller than for animals implanted with RHA or RTCP (Fig. 5g, i, k). In animals without implantation at 24 weeks after creation of the bone defect, TRAP-positive cells were detected on the surface of newly formed bone, but the activity was much less than that of animals without implantation at 4 weeks after creation of the bone defect (Fig. 5g, h). TRAP-positive multinucleated cells were detected abundantly in animals implanted with RHA at 24 weeks after implantation. Not only the number of TRAP-positive multinucleated cells, but also the TRAP activity in individual cells, was not clearly different from that of animals at 4 weeks after implantation of RHA (Fig. 5i, j). In animals at 24 weeks after implantation of RTCP, the TRAP activity in individual cells was similar to that in animals at 4 weeks after implantation of RTCP, but the number of TRAP-positive multinucleated cells tended to be reduced (Fig. 5k, l).

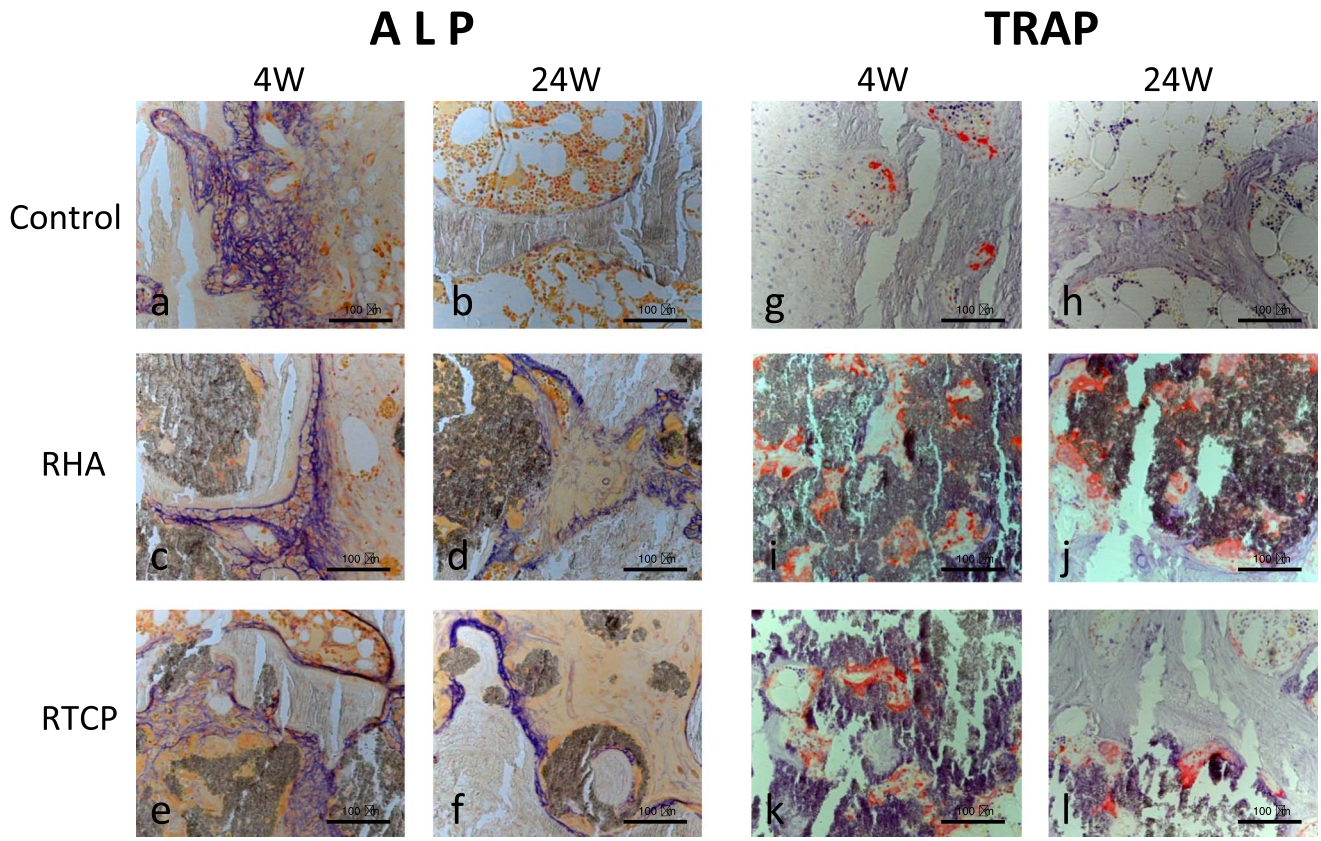

Fig. 5. Expression profiles of the activities of ALP and TRAP in specimens at 4 and 24 weeks after implantation or creation of bone defects. The expression of ALP (**a, b**) and TRAP (**g, h**) in rat femurs without implantation at 4 weeks (**a, g**) and 24 weeks (**b, h**) after creation of the bone defect. The expression of ALP (**c, d**) and TRAP (**i, j**) in rat femurs implanted with RHA at 4 weeks (**c, i**) and 24 weeks (**d, j**) after implantation. The expression of ALP (**e, f**) and TRAP (**k, l**) in rat femurs implanted with RTCP at 4 weeks (**e, k**) and 24 weeks (**f, l**) after implantation. The activity of ALP was stained with purple in the membrane of osteoblasts, and the activity of TRAP was stained with red in osteoclasts.

Histomorphometry

[BV + Imp.V]/TV of animals implanted with RHA or RTCP was significantly higher than that of animals without implantation, which was because of an absence of Imp.V in animals without implantation. [BV + Imp.V]/TV of animals implanted with RHA remained around 70 and 80%, and an increasing tendency at 24 weeks after implantation was seen. [BV + Imp.V]/TV of animals implanted with RTCP remained around 70% and did not clearly change throughout the experimental period (Fig. 6A). At 24 weeks after implantation, [BV + Imp.V]/TV of animals implanted with RHA was significantly higher than that of animals implanted with RTCP.

The amount of residual bone substitutes was quantitated using the parameter Imp.V/TV. Imp.V/TV of RHA tended to be higher than that of RTCP throughout the experimental period, but the difference was not significant except for at 8 weeks after implantation. Chronological change of Imp.V/TV was also analyzed. Reduced tendency of Imp.V/TV was seen in both RHA and RTCP, but was not obvious (Fig. 6B). Significant reduction of the amount of HHA was detected at 12 weeks after implantation when compared with that at 4 weeks after implantation, but the others were not significant (Fig. 7A).

BV/TV was compared among animals implanted with RHA, RTCP and animals without implantation in the bone defect. Between animals implanted with RHA and RTCP, and animals implanted with RTCP and without implantation in the bone defect, BV/TV was not significantly different throughout the experimental period. In animals without implantation in the bone defect, relatively high BV/TV was detected at 8 weeks after creation of the bone defect, and was significantly higher than that of animals implanted with RHA. However, BV/TV tended to be reduced at 12 and 24 weeks after creation of the bone defect, and was significantly lower than that of animals implanted with RHA at 24 weeks after implantation (Fig. 6C). Chronological change of BV/TV was analyzed, and 12 and 24 weeks after implantation, BV/TV of animals implanted with RHA was significantly higher than that of animals at 4 weeks after

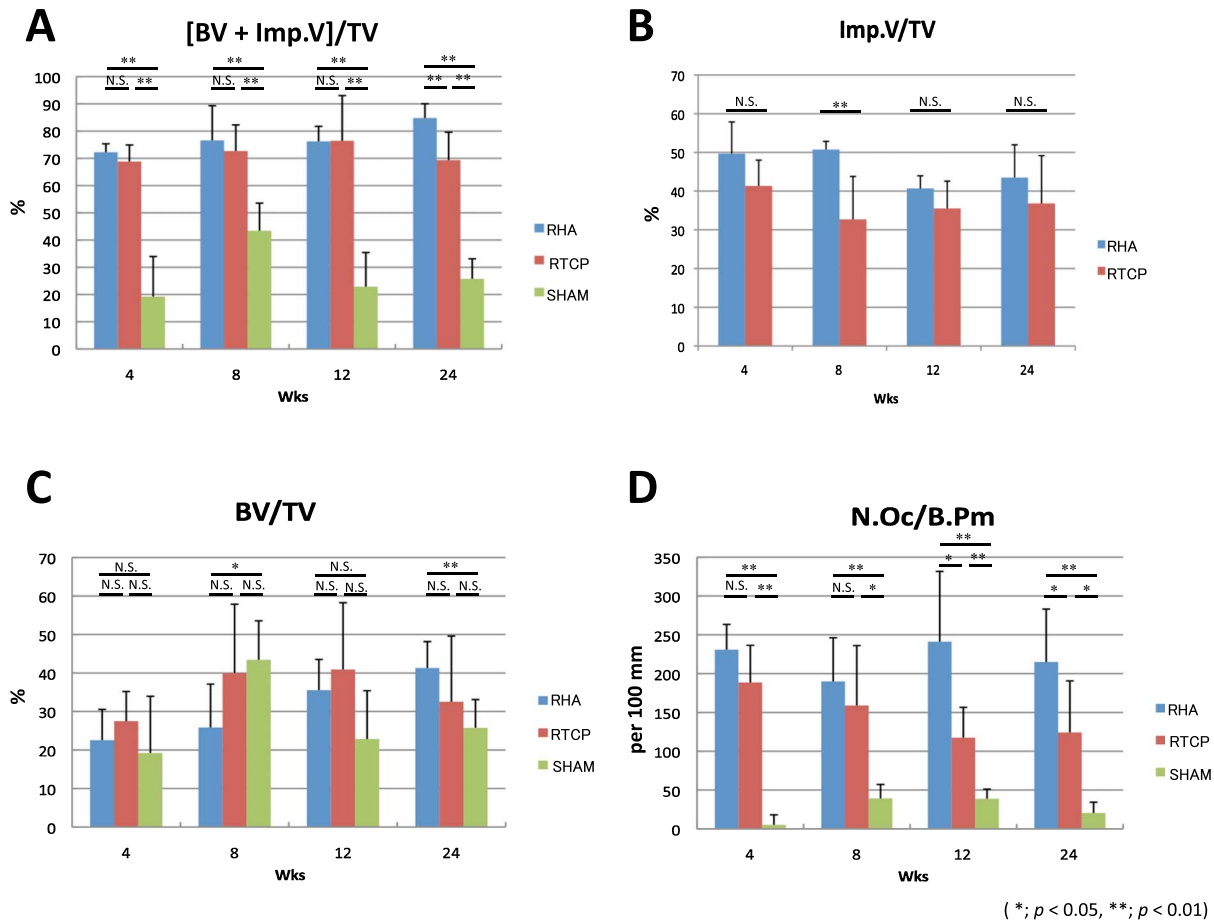

Fig. 6. Histomorphometric quantitations of implants and bones in specimens and comparison among each experimental group at 4, 8, 12 and 24 weeks after implantation or creation of bone defects. Parameters of the amount of total hard tissue volume including the amount of implants and newly formed bone over the amount of total tissue, [BV + Imp.V]/TV (**A**), the net amount of implants over the amount of total tissue, Imp.V/TV (**B**), and the net amount of newly formed bone over the amount of total tissue, BV/TV (**C**), were evaluated. A parameter for osteoclasts, N.Oc/B.Pm (**D**), was also compared. Six samples for each experiment were analyzed for the acquired data. *P<0.05, **P<0.01.

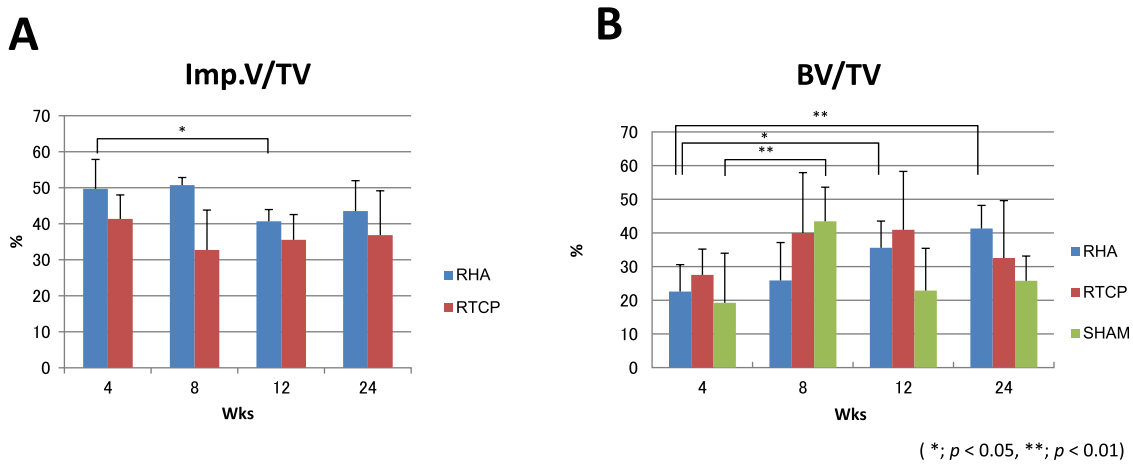

Fig. 7. Histomorphometric quantitations of implants and bones in specimens and comparison of the chronological change in each experimental group. The net amount of implants over the amount of total tissue, Imp.V/TV (**A**), and the net amount of newly formed bone over the amount of total tissue, BV/TV (**B**), were evaluated. Six samples for each experiment were analyzed for the acquired data. *P<0.05, **P<0.01.

implantation (Fig. 7B). In animals without implantation, BV/TV at 8 weeks after implantation was significantly higher than that at 4 weeks after implantation, but was reduced at 12 and 24 weeks after implantation (Fig. 7B).

In animals without implantation, N.Oc/B.Pm was much smaller than those of animals implanted with RHA or RTCP throughout the experimental period. In animals implanted with RHA, N.Oc/B.Pm remained large throughout the experimental period. In contrast, N.Oc/B.Pm in animals implanted with RTCP tended to be reduced at 12 and 24 weeks after implantation, and N.Oc/B.Pm in animals implanted with RHA was significantly larger than that of animals implanted with RTCP at 12 and 24 weeks after implantation (Fig. 6D).

IV. Discussion

Mechanical unloading has been shown to reduce bone mass during a short period [10, 21, 28], and radiological findings and measurements of the length and width of right tibiae with and without sciatic neurectomy confirmed that loss of bone mass and growth inhibition occurred in animals with sciatic neurectomy during 2 weeks (Fig. 3B, C). No significant change of the length of tibiae was seen at 24 weeks after creation of the bone defect (Fig. 3C, a). This was explained by age-dependent reduction of the activity of the growth plate. In animals at 24 weeks after creation of the bone defect, sciatic neurectomy was performed at 22 weeks after creation of the bone defect, and animals were 30 weeks of age. At that age, the growth plate of the rat was atrophied and was thought to have weak activity. Thus, further increase in the length of tibiae was not expected.

It was remarkable that the activities of ALP in osteoblasts and TRAP in osteoclasts in regions implanted with either RHA or RTCP were much stronger than those in regions of bone defects without implantation at 24 weeks after implantation or creation of the bone defect (Fig. 5). Cuboidal shape of osteoblasts with strong ALP activity (Fig. 5d, f) suggested that RHA and RTCP stimulated total activity of osteoblasts in the implanted region. Postmenopausal osteoporosis is induced by decreased activity of estrogen, which leads to stimulation of bone resorption. In contrast, the reduction in bone under mechanical unloading is thought to be largely associated with decreased activity of osteoblasts [10, 24, 26], and stimulation of osteoblasts is expected to contribute to prevent the bone reduction. Interestingly, BV/TV in regions implanted with RHA was significantly higher at 12 and 24 weeks than that at 4 weeks after implantation, but that in regions implanted with RTCP was not significantly different at any stages (Fig. 7B). Previously, we reported that RHA possessed a stimulatory effect on osteogenesis with potent osteoclast-homing performance when implanted into bone defects [11, 31], and these findings suggested that both RHA and RTCP stimulated osteoblast activity, but only RHA effectively improved repair of bone defects under mechanical unloading by its potent stimulatory effect on osteogenesis. The potent stimulation of osteogenesis by RHA might contribute to improve repair of bone defects in patients under conditions of skeletal unloading, including those with long-term bed rest and astronauts.

The mechanism of the stimulatory effect of osteogenesis by RHA is uncertain. Crosstalk between osteoblasts and osteoclasts has long been discussed and the expression of receptor activator of nuclear factor-κB ligand (RANKL) in osteoblasts was found to be essential to osteoclastogenesis [5]. Recently, semaphorin 3A, which is expressed by osteoblasts, was shown to inhibit osteoclast differentiation of bone marrow cells and also had a potent stimulatory effect on osteogenesis [13]. In turn, some molecules expressed in osteoclasts were also shown to regulate osteogenesis. Cardiotrophin-1, a cytokine expressed by osteo-

clasts, has been reported to stimulate osteogenesis [42]. Semaphorin 4D expressed in osteoclasts was shown to inhibit osteogenesis. Mice that lack semaphorin 4D revealed an osteosclerotic phenotype [9, 29]. We previously suggested that osteoclasts cultured on RHA expressed certain soluble factors that stimulate osteoblast differentiation [11]. N.Oc/B.Pm in regions implanted with RHA was significantly larger than that in regions implanted with RTCP at 12 and 24 weeks after implantation (Fig. 6D), and osteoclasts on the surface of implanted RHA might express a certain stimulator of osteogenesis *in vivo*. It has been reported that the surface microstructure of implants affected the differentiation of osteogenic cells [25, 39]. Kitazawa and Kitazawa reported that, in tumor-induced osteolytic lesions, not only osteoblasts but also stromal cells between cancer cells expressed RANKL [20]. Although the stromal cells were not characterized in that report, they might be osteoblast progenitor cells differentiated from bone marrow mesenchymal stem cells under the influence of cancer cells. We do not have any evidence here, but there is also the possibility that RHA itself possesses a stimulatory effect on osteogenesis by its unique rod-shaped microstructure, and contributes to differentiate bone marrow mesenchymal stem cells into osteoblasts.

In this study, potent osteoclast-homing performance of RHA was confirmed to be retained after 2 weeks of mechanical unloading. A direct effect of mechanical unloading on osteoclastogenesis or the activity of osteoclasts remains uncertain. Recently, osteocytes, which were embedded into the bone matrix, were shown to play a key role in regulating bone loss induced by mechanical unloading. Without expression of one of the key osteoclastogenic factors, RANKL in osteocytes, significant reduction of bone mass was not seen, even after mechanical unloading [45]. It was also reported that significant reduction of bone mass was not seen after mechanical unloading in mice that lack osteocytes [36]. The mechanism of potent osteoclast homing by RHA remains unclear, but there are no osteocytes in bone substitutes and it should be osteocyte independent. It might be associated with the rod-shaped microstructure of the ceramic particles or there might be certain molecules preferentially adsorbed in RHA that associate with osteoclast homing and/or osteoclastogenesis. In addition, Imp.V/TV of RHA and RTCP was not obviously reduced during the experimental period, and this may be explained by the absence of osteocytes in bone substitutes.

V. Acknowledgments

We thank Toshiharu Takahashi of Tohoku University for preparation of ceramic samples, Hisashi Murayama of Kureha Special Laboratory for technical assistance and advice on sciatic neurectomy, and Dr. Yasuhiro Kumei of Tokyo Medical and Dental University for advice on mechanical unloading. This work was supported in part by Grants-in-Aid from the Ministry of Education, Culture, Sports and Technology of Japan (Grant nos. 22390343 and 21300175) and Ground-based Research Program for Space Utilization promoted by the Japan Space Forum.

VI. References

1. Anker, C. J., Holdridge, S. P., Baird, B., Cohen, H. and Damron, T. A. (2005) Ultraporous beta-tricalcium phosphate is well incorporated in small cavitary defects. *Clin. Orthop. Relat. Res.* 434; 251–257.
2. Apseloff, G., Girten, B., Weisbrode, S. E., Walker, M., Stern, L. S., Krecic, M. E. and Gerber, N. (1993) Effects of aminohydroxybutane bisphosphonate on bone growth when administered after hind-limb bone loss in tail-suspended rats. *J. Pharmacol. Exp. Ther.* 267; 515–521.
3. Bateman, T. A., Zimmerman, R. J., Ayers, R. A., Ferguson, V. L., Chapes, S. K. and Simske, S. J. (1998) Histomorphometric, physical, and mechanical effects of spaceflight and insulin-like growth factor-I on rat long bones. *Bone* 23; 527–535.
4. Bikle, D. D., Morey-Holton, E. R., Doty, S. B., Currier, P. A., Tanner, S. J. and Halloran, B. P. (1994) Alendronate increases skeletal mass of growing rats during unloading by inhibiting resorption of calcified cartilage. *J. Bone Miner. Res.* 9; 1777–1787.
5. Boyle, W. J., Simonet, W. S. and Lacey, D. L. (2003) Osteoclast differentiation and activation. *Nature* 423; 337–342.
6. Bucholz, R. W., Carlton, A. and Holmes, R. (1989) Interporous hydroxyapatite as a bone graft substitute in tibial plateau fractures. *Clin. Orthop. Relat. Res.* 240; 53–62.
7. Carmeliet, G., Vico, L. and Bouillon, R. (2001) Space flight: a challenge for normal bone homeostasis. *Crit. Rev. Eukaryot. Gene Expr.* 11; 131–144.
8. Cullinane, D. M. (2002) The role of osteocytes in bone regulation: mineral homeostasis versus mechanoreception. *J. Musculoskelet. Neuronal Interact.* 2; 242–244.
9. Dacquin, R., Domenget, C., Kumanogoh, A., Kikutani, H., Jurdic, P. and Machuca-Gayet, I. (2011) Control of bone resorption by semaphorin 4D is dependent on ovarian function. *PLoS One* 6; e26627.
10. Globus, R. K., Bikle, D. D. and Morey-Holton, E. (1986) The temporal response of bone to unloading. *Endocrinology* 118; 733–742.
11. Gonda, Y., Ioku, K., Shibata, Y., Okuda, T., Kawachi, G., Kamitakahara, M., Murayama, H., Hideshima, K., Kamihira, S., Yonezawa, I., Kurosawa, H. and Ikeda, T. (2009) Stimulatory effect of hydrothermally synthesized biodegradable hydroxyapatite granules on osteogenesis and direct association with osteoclasts. *Biomaterials* 30; 4390–4400.
12. Goto, T., Kojima, T., Iijima, T., Yokokura, S., Kawano, H., Yamamoto, A. and Matsuda, K. (2001) Resorption of synthetic porous hydroxyapatite and replacement by newly formed bone. *J. Orthop. Sci.* 6; 444–447.
13. Hayashi, M., Nakashima, T., Taniguchi, M., Kodama, T., Kumanogoh, A. and Takayanagi, H. (2012) Osteoprotection by semaphorin 3A. *Nature* 485; 69–74.
14. Hoogendoorn, H. A., Renooij, W., Akkermans, L. M., Visser, W. and Wittebol, P. (1984) Long-term study of large ceramic implants (porous hydroxyapatite) in dog femora. *Clin. Orthop. Relat. Res.* 187; 281–288.
15. Ikeda, T., Kasai, M., Suzuki, J., Kuroyama, H., Seki, S., Utsuyama, M. and Hirokawa, K. (2003) Multimerization of the receptor activator of nuclear factor-kappaB ligand (RANKL) isoforms and regulation of osteoclastogenesis. *J. Biol. Chem.* 278; 47217–47222.
16. Ioku, K., Kawachi, G., Yamasaki, M., Toda, H., Fujimori, H. and Goto, S. (2005) Hydrothermal preparation of porous hydroxyapa-

tite with tailrod crystal surface. *Key Eng. Mater.* 288–289; 521–524.
17. Ioku, K., Kamitakahara, M., Kawachi, G., Gonda, Y., Okuda, T., Yonezawa, I., Kurosawa, H. and Ikeda, T. (2008) Microstructure designing of porous β-tricalcium phosphate for control of reactions in the bone. *Key Eng. Mater.* 361–363; 989–992.
18. Irie, K., Ozawa, H. and Yajima, T. (2000) The histochemical and cytochemical changes from formative to resorptive osteocytes. *Acta Histochem. Cytochem.* 33; 385–391.
19. Keila, S., Pitaru, S., Grosskopf, A. and Weinreb, M. (1994) Bone marrow from mechanically unloaded rat bones expresses reduced osteogenic capacity in vitro. *J. Bone Miner. Res.* 9; 321–327.
20. Kitazawa, R. and Kitazawa, S. (2005) In situ hybridization on calcified tissue: Detection of RANKL mRNA in mouse osteolytic bone lesions. *Acta Histochem. Cytochem.* 38; 143–149.
21. Kodama, Y., Nakayama, K., Fuse, H., Kurokawa, T., Nakamura, T. and Matsumoto, T. (1999) Changes in bone tissue of tail-suspended rats. In "Mechanical Loading of Bones and Joints" ed. by H. E. Takahashi, Springer, Tokyo, pp. 115–122.
22. Komaki, H., Tanaka, T., Chazono, M. and Kikuchi, T. (2006) Repair of segmental bone defects in rabbit tibiae using a complex of beta-tricalcium phosphate, type I collagen, and fibroblast growth factor-2. *Biomaterials* 27; 5118–5126.
23. LeGeros, R. Z. (2002) Properties of osteoconductive biomaterials: calcium phosphates. *Clin. Orthop. Relat. Res.* 395; 81–98.
24. Machwate, M., Zerath, E., Holy, X., Hott, M., Modrowski, D., Malouvier, A. and Marie, P. J. (1993) Skeletal unloading in rat decreases proliferation of rat bone and marrow-derived osteoblastic cells. *Am. J. Physiol.* 264; E790–799.
25. Mendonca, D. B., Miguez, P. A., Mendonca, G., Yamauchi, M., Aragao, F. J. and Cooper, L. F. (2011) Titanium surface topography affects collagen biosynthesis of adherent cells. *Bone* 49; 463–472.
26. Morey, E. R. and Baylink, D. J. (1978) Inhibition of bone formation during space flight. *Science* 201; 1138–1141.
27. Murakami, H., Nakamura, T., Tsurukami, H., Abe, M., Barbier, A. and Suzuki, K. (1994) Effects of tiludronate on bone mass, structure, and turnover at the epiphyseal, primary, and secondary spongiosa in the proximal tibia of growing rats after sciatic neurectomy. *J. Bone Miner. Res.* 9; 1355–1364.
28. Nakamura, T., Sakata, K., Tsurukami, H. and Sakai, A. (1999) Mechanical unloading and bone marrow cells. In "Mechanical Loading of Bones and Joints", ed. by H. E. Takahashi, Springer, Tokyo, pp. 105–113.
29. Negishi-Koga, T., Shinohara, M., Komatsu, N., Bito, H., Kodama, T., Friedel, R. H. and Takayanagi, H. (2011) Suppression of bone formation by osteoclastic expression of semaphorin 4D. *Nat. Med.* 17; 1473–1480.
30. Okuda, T., Ioku, K., Yonezawa, I., Minagi, H., Kawachi, G., Gonda, Y., Murayama, H., Shibata, Y., Minami, S., Kamihira, S., Kurosawa, H. and Ikeda, T. (2007) The effect of the microstructure of beta-tricalcium phosphate on the metabolism of subsequently formed bone tissue. *Biomaterials* 28; 2612–2621.
31. Okuda, T., Ioku, K., Yonezawa, I., Minagi, H., Gonda, Y., Kawachi, G., Kamitakahara, M., Shibata, Y., Murayama, H., Kurosawa, H. and Ikeda, T. (2008) The slow resorption with replacement by bone of a hydrothermally synthesized pure calcium-deficient hydroxyapatite. *Biomaterials* 29; 2719–2728.
32. Parfitt, A. M., Drezner, M. K., Glorieux, F. H., Kanis, J. A., Malluche, H., Meunier, P. J., Ott, S. M. and Recker, R. R. (1987) Bone histomorphometry: standardization of nomenclature, symbols, and units. Report of the ASBMR Histomorphometry Nomenclature Committee. *J. Bone Miner. Res.* 2; 595–610.
33. Rabin, R., Gordon, S. L., Lymn, R. W., Todd, P. W., Frey, M. A. and Sulzman, F. M. (1993) Effects of spaceflight on the musculoskeletal system: NIH and NASA future directions. *FASEB J.* 7; 396–398.
34. Suzue, N., Nikawa, T., Onishi, Y., Yamada, C., Hirasaka, K., Ogawa, T., Furochi, H., Kosaka, H., Ishidoh, K., Gu, H., Takeda, S., Ishimaru, N., Hayashi, Y., Yamamoto, H., Kishi, K. and Yasui, N. (2006) Ubiquitin ligase Cbl-b downregulates bone formation through suppression of IGF-I signaling in osteoblasts during denervation. *J. Bone Miner. Res.* 21; 722–734.
35. Takahashi, T., Kamitakahara, M., Kawachi, G. and Ioku, K. (2008) Preparation of spherical porous granules composed of rod-shaped hydroxyapatite and evaluation of their protein adsorption properties, *Key Eng. Mater.* 361–363; 83–86.
36. Tatsumi, S., Ishii, K., Amizuka, N., Li, M., Kobayashi, T., Kohno, K., Ito, M., Takeshita, S. and Ikeda, K. (2007) Targeted ablation of osteocytes induces osteoporosis with defective mechanotransduction. *Cell Metab.* 5; 464–475.
37. Turner, R. T., Evans, G. L. and Wakley, G. K. (1995) Spaceflight results in depressed cancellous bone formation in rat humeri. *Aviat. Space Environ. Med.* 66; 770–774.
38. Uusitalo, H., Rantakokko, J., Vuorio, E. and Aro, H. T. (2005) Bone defect repair in immobilization-induced osteopenia: a pQCT, biomechanical, and molecular biologic study in the mouse femur. *Bone* 36; 142–149.
39. Valencia, S., Gretzer, C. and Cooper, L. F. (2009) Surface nanofeature effects on titanium-adherent human mesenchymal stem cells. *Int. J. Oral Maxillofac. Implants* 24; 38–46.
40. Vandamme, K., Holy, X., Bensidhoum, M., Logeart-Avramoglou, D., Naert, I. E., Duyck, J. A. and Petite, H. (2011) In vivo molecular evidence of delayed titanium implant osseointegration in compromised bone. *Biomaterials* 32; 3547–3554.
41. Verhaeghe, J., Thomsen, J. S., van Bree, R., van Herck, E., Bouillon, R. and Mosekilde, L. (2000) Effects of exercise and disuse on bone remodeling, bone mass, and biomechanical competence in spontaneously diabetic female rats. *Bone* 27; 249–256.
42. Walker, E. C., McGregor, N. E., Poulton, I. J., Pompolo, S., Allan, E. H., Quinn, J. M., Gillespie, M. T., Martin, T. J. and Sims, N. A. (2008) Cardiotrophin-1 is an osteoclast-derived stimulus of bone formation required for normal bone remodeling. *J. Bone Miner. Res.* 23; 2025–2032.
43. Weinreb, M., Rodan, G. A. and Thompson, D. D. (1989) Osteopenia in the immobilized rat hind limb is associated with increased bone resorption and decreased bone formation. *Bone* 10; 187–194.
44. Weinreb, M., Rodan, G. A. and Thompson, D. D. (1991) Depression of osteoblastic activity in immobilized limbs of suckling rats. *J. Bone Miner. Res.* 6; 725–731.
45. Xiong, J., Onal, M., Jilka, R. L., Weinstein, R. S., Manolagas, S. C. and O'Brien, C. A. (2011) Matrix-embedded cells control osteoclast formation. *Nat. Med.* 17; 1235–1241.